

Bayesian network based probabilistic model for optimized inspection intervals for offshore wind turbine support structures

M.P. Nicoreac, W.M.G. Courage, P.L. Kempker

Netherlands Institute of Applied Scientific Research (TNO), the Netherlands

The support structures of offshore wind turbines (OWTs) are difficult to inspect due to the environmental conditions and difficult access to structural parts. The inspection and maintenance cost are therefore high, providing a good motivation for further optimizing the planning and costs for these actions. In the context of the FeLoSeFI project, a risk based concept is used in which the uncertainties in fatigue life prediction models are considered. The probability of failure versus the costs of maintenance provide a good picture of the consequences regarding the maintenance actions to be applied.

Key words: Risk based inspection, maintenance, optimization, OWT, Bayesian networks

1 Introduction

Probabilistic models are frequently used for life cycle assessments of different type of structures such as bridges and offshore wind turbines, where the reliability of these structures is a critical issue. Multiple welded details in offshore wind turbines (OWTs) support structures are prone to deterioration due to fatigue loading. Environmental and accessibility conditions make inspection and maintenance for OWT's costly. With fatigue as a driver for these actions, a gain is to be found in optimizing the planning of these actions. Hence the development of an optimization tool which is based on probabilistic methods. The tool exploits a Dynamic Bayesian Network (DBN) methodology introduced by [Straub, 2009] and an application to OWT proposed by [Nielsen and Sørensen, 2011]. This risk based concept balances the probabilities of failure and its consequences against costs of inspections and actions, including different inspection and maintenance methods, taking uncertainties into account. This approach fits with a recent recommended practice on planning of inspections by [DNV-GL, 2015].

2 Bayesian Networks as probabilistic prediction models

The use of probabilistic models for the detectability of defects and for fatigue crack growth in welded structures has been the point of interest of various research [Chryssanthopoulos and Righiniotis, 2006; J Maljaars et al., 2012]. Probabilistic fatigue assessment models for welded structures can have two types of approaches for formulating the fatigue limit state: one based on S-N curves and damage accumulation rules, while the other approach is based on Fracture Mechanics (FM). The latter approach is used in the FeLoSeFI project due to the possibility of determining inspection intervals.

Bayesian techniques have been used in the recent years for the probabilistic fatigue assessment of various structures. The advantage of using Bayesian Networks (BN) consists of the possibility to update the parameters in the model as soon as new information or results are available. By considering results from inspection and monitoring, such as measured crack sizes, absence of cracks and load history, the existing probabilistic model can be improved. BN can quantify the consequences on the reliability of the structure due to new information.

2.1 *Bayesian networks general information*

Bayesian networks (BNs) are tools for reasoning and decision making based on expectations and probability distributions, in situations where the state variables are stochastic and unobserved [Kjaerulff and Madsen, 2008].

In the context of this research, Bayesian Networks are used to find the optimal inspection intervals and repair decisions, given the inherent trade-off between inspection/repair costs and expected costs of failure. When an inspection is performed, the uncertainty about the size of a crack in that location decreases. Given this more accurate information, the decision to repair the crack is taken if a value exceeding a given threshold is detected. The decision whether or not to do an inspection involves weighting the value of more accurate information (i.e. the impact of this information on the expected cost of failure, given the possible repair action) against the cost of inspection (which in the case of offshore windmills is quite high).

2.2 *Limited memory influence diagram*

Despite developments with respect to the modelling of continuous variables, common methods to represent variables in a BN use discrete approximations. This means that the computational complexity of a BN hinges on having a few distinct discrete values per variable, but enough distinct values needed for the model to remain a meaningful representation of the problem. The nodes in a BN are represented by variables that are relationally connected by directed arcs. The relationship is represented by conditional probability tables (CPTs). The CPT of a node N is represented by a table which collects the conditional probabilities of all possible discrete values of N , for each possible combination of discrete values of all nodes with an arc ending in N .

Figure 1 gives the schematic representation of the BN topology used in this research and whose variables will be described in section 3. A specific type of BN is represented, called an influence diagram (ID), which includes utility nodes (diamond shaped in Figure 1), decision nodes (box shaped) and chance nodes for the variables (circular shaped), with directed arcs that make up for the basic BN. With respect to the basic BN that can only provide information about the probability of a certain event taking place, the introduction of utility and decision nodes makes it possible to quantify utilities (costs) as well as to decide on scenarios with respect to actions to be taken based on a given evidence. By introducing decision nodes in a BN, the impact of different decisions on the probability distribution of future variables can be determined. If these decision nodes are linked to utility nodes, then the expected utilities corresponding to different decisions can be compared with each other. The consequences of (combinations of) different choices can be analysed in this way and the optimal strategies can be found, i.e. rules that determine the optimal decisions or combinations of decisions for all possible situations.

The problem with optimizing the maintenance decisions for many consecutive years is the dependence of the decision on all previous information and decision. This leads to a large number of possible strategies. To overcome this problem a limited memory influence diagram (LIMID) is used [Lauritzen and Nilsson, 2001]. For the BN considered in this research the decisions are based on some recent variables, while all other past information and decisions are neglected or forgotten. With respect to the BN framework this implies that the decision nodes can only take information from direct parent nodes.

2.3 Policies and strategies for the influence diagram (ID)

The optimal decision policy for an influence diagram (ID) is found for every decision node by considering all previous probability and decision nodes. For large networks finding the optimal decision policy can be an unmanageable problem. This has to do with the decisions that need to be made which are based on policies for future decisions so that expected utilities can be calculated. These expected utilities are used to obtain the optimal policies for a current decision. The domain of a decision node grows exponentially with the number of previous nodes.

The optimal strategy for a LIMID can be found by using single policy updating (SPU) algorithm [Lauritzen and Nilsson, 2001]. Beginning with a set of policies (or – equivalent – strategies), this iterative algorithm picks one policy at a time, and checks whether a better overall result can be achieved by making changes to that policy. If no better result can be achieved by changing any one policy anymore, the algorithm terminates. This results in a local optimum; for a global optimum it would be necessary to also check whether changing several policies simultaneously would lead to better results, at a much higher computational expense.

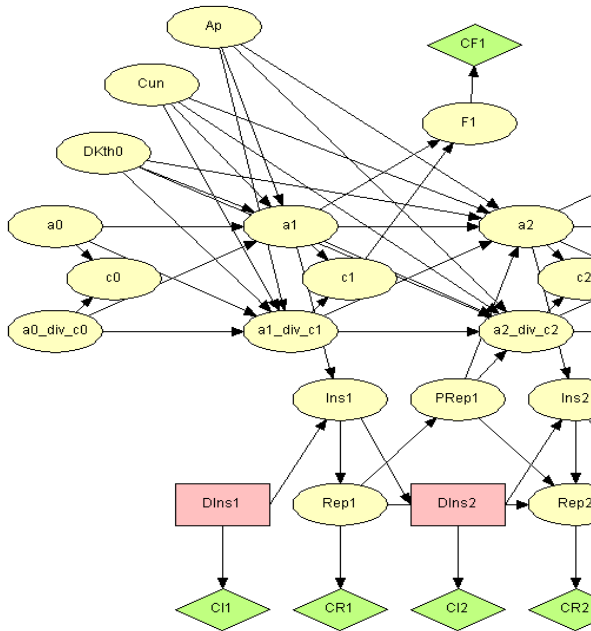


Figure 1: Topology of BN network used in current research
(See section 3 for the description of the variables.)

3 Belief net used in the current research

The degradation of steel components of OWTs is modelled using Bayesian Networks as presented in the previous section. The expected lifetime is modelled with 20 time steps of one year. The size of the time steps was chosen to correspond with the timeframe and seasonality of the maintenance work.

Figure 1 shows all variables and their connections in the first time step (year 1). The nodes on the left represent the input variables of the network. Two types of variables can be distinguished: initial state variables and external model parameters.

The initial state variables have influence only on the state variables of year 1 and those in turn influence the state variables of year 2, and so on. The initial state variables considered in the BN together with the distribution assumed for each variable are described here below:

- a_0 Indicates the initial crack depth in mm and is represented by a log-normally distributed random variable. For the current BN model a_0 is discretized into 7 states (see Table 1);
- c_0 Indicates the initial crack half width in mm; instead of defining a marginal distribution for c_0 , the distribution from the initial crack depth c_0 and the initial aspect ratio a_0/c_0 is derived. With this choice, the constraint $a_0/c_0 > 0$ from the fracture mechanics model can be incorporated in a straightforward way;
- The initial aspect ratio a_0/c_0 is modelled as a log-normally distributed random variable. Due to the lack of crack growth models for initial aspect ratios higher than 2, a cut-off is provided at 2. Both c_0 and a_0/c_0 are discretized into 7 discrete states, similar to a_0 (see Table 1).

The distribution types together with the distribution parameters of the initial state variables are taken according to [Faber and Vrouwenvelder, 2001], and presented in Table 2.

The external model parameters are time-invariant, i.e. their value remains the same for each year. These detail or hotspot specific parameters directly influence the state variables for all years. The following external model parameters are considered in the Bayesian network in this research:

- A material-specific constant A_p relates the crack growth rate (crack extension per cycle) to the stress intensity range ΔK . Its logarithm $\log_{10}(A_p)$ is modelled as a normally distributed random variable
- The threshold value ΔK_{th} for the stress intensity range ΔK is represented by a log-normally distributed random variable
- The model uncertainty parameter C_{un} is log-normally distributed

Table 1: Discretization of a_0 and c_0 in 7 states

State	a_0 min	a_0 max	a_0 min	a_0 max	$(a_0 / c_0)_{min}$	$(a_0 / c_0)_{max}$
-	mm	mm	mm	mm	-	-
1	0.00	0.05	0.00	0.05	0.00	0.22
2	0.05	0.09	0.05	0.09	0.22	0.32
3	0.09	0.17	0.09	0.17	0.32	0.47
4	0.17	0.31	0.17	0.31	0.47	0.70
5	0.31	1.00	0.31	1.00	0.70	1.03
6	1.00	25.00	1.00	25.00	1.03	1.52
7	25.00	100.00	25.00	100.00	1.52	2.00

The distribution and distribution parameters of the external model parameters A_p and ΔK_{th} depend on the environment in which the detail is located (air or marine environment). Recommendations are provided in [BS7910:2013, 2015] and [Faber and Vrouwenvelder, 2001] regarding the distribution type and parameters of A_p and ΔK_{th} for steels, depending on the environment and stress ratio R . Another approach is to perform material tests to determine the material constants A_p and ΔK_{th} . The distribution and distribution parameters of the model uncertainty in this paper are taken according to [Faber and Vrouwenvelder, 2001] and presented in Table 2.

3.1 Structure of the Bayesian belief network

Starting from the initial state variables a_0 and c_0 and the model parameters of the crack growth model used to simulate the degradation of the considered detail, the distribution of the state variables in the first year, a_1 and c_1 are determined. The aspect ratio a_1 / c_1 is used as an auxiliary state variable to incorporate the constraints related to it.

Based on the distribution of a_1 and c_1 , the failure probability in the first year can be obtained. Failure in this case is defined by the failure of the structure conditional to the

Table 2: Variables in the damage model and their distribution [Faber and Vrouwenvelder, 2001]

Variable	Distribution	Mean η	Standard deviation σ	Unit
a_0	lognormal	0.15	0.10	mm
a_0/c_0	lognormal	0.62	0.25	-
$\log_{10}(A_p)$	lognormal	1)	1)	-
ΔK_{th}	lognormal	1)	1)	N/mm ^{1.5}
C_{un}	lognormal	1.00	0.27	-

1) Depends on the environment and stress ratio R , see examples.

failure of the considered detail (hot-spot) and is described in node F_1 of the BN (see Figure 1). The importance of the hot spot is taken into account by the relative importance factor (RIF). For the examples presented in this paper, the annual probability of failure is quantified as 0.0086 for crack sizes in state 7 (Table 1). This corresponds to a 20 years reliability index of 1 conditional on the detail being failed. For states 1 to 5 the 20 years reliability index is set to 3 whereas in state 6 this index corresponds to the intermediate value of 2.

The cost of failure, which is interpreted as negative utility, is provided by the utility node CF1. This node will return the cost of failure if the value of node F_1 is 'failure' and 0 otherwise. The cost of failure is assumed in this research to be equivalent to the investment cost for one wind turbine.

3.2 Inspection and repairs considered in the Bayesian belief network

The decision whether to perform an inspection at time step t (year t) is provided by the decision node $DIns_t$. Starting from the second year, node $DIns_t$ is connected to the inspection node Ins_{t-1} of the previous year, so that the decision about inspections for year t takes into account the outcome of the previous year. There are three types of inspections possible in the belief net described in this paper:

- Eddy current (EC), magnetic particle inspection (MPI) and alternating current field measurements (ACFM) with cost C_{ins1} ;
- Ultrasonic (UT) with cost C_{ins2} ;
- Visual inspection with cost C_{ins3} .

The probability that a defect is found during an inspection is determined by the defect size (depth a or length $2c$) and the inspection technique. This relationship is expressed in the form of a probability of detection (PoD) curve that differs per inspection method. Also for a certain inspection method there is a differentiation in the accessibility of the inspected detail. Information about performed inspections can be included in the node Ins_t which has three possibilities: 'no inspection', 'no detection' or a discrete value for the detected crack size. If at one time step t (year t), an inspection is performed and a crack is detected, than the inspection accuracy is modelled by assigning the correct discrete value of the crack size a_t with a likelihood of 0.8 times the PoD of a_t , and a discrete value which is by one step too high or too low respectively with a likelihood of 0.1 times the PoD of a_t each. If an inspection is performed but no crack was found, than this event is assigned with a likelihood of $1 - PoD$ as a function of a_t . The PoD is dependent on the crack depth a in the case of EC/MPI/ACFM and UT inspection techniques while for the visual inspection the PoD is dependent on the length of the defect $2c$. The PoD curve for the EC/MPI/ACFM and UT inspection techniques is provided in [DNV-GL, 2015]:

$$PoD(a) = 1 - \frac{1}{1 + \left(\frac{a}{X_0}\right)^b} \quad (1)$$

were a is the crack depth in mm (or crack length in mm, for the case of visual inspection), X_0 and b are distribution parameters. These are presented in Table 3. The assumption regarding the conditions of the inspections is that these are performed below water or in less good working conditions above water.

Table 3: PoD curve parameters for different inspection techniques and the accessibility considered in this research [DNV-GL, 2015]

Inspection technique and accessibility	X_0 [mm]	b [-]
EC/MPI/ACFM – Below water and less good working conditions above water	1.16	0.900
UT – AI qualifications and execution of work	0.41	0.642
Visual – Difficult access	83.03	1.079

The decision to perform a repair action is included in the decision node Rep_t and depends on inspection result of the previous year and – if applicable – on the repair decision of the previous year. The following rules are used for the repair decision:

- If a repair action in the previous year was unsuccessful, the same repair action is chosen again, regardless of the inspection outcome
- Otherwise, if a crack depth between 0.31 mm and 1 mm is detected, a minor repair is chosen, and if a crack depth above 1 mm is detected, a major repair is chosen
- In all other cases it is decided not to repair a possible crack

The costs of the different types of inspections and the cost of repairs are considered as negative utilities in the utility nodes CI_t and $CRep_t$ respectively. The cost of inspection for one detail is estimated by considering a total cost for inspecting several joints in one day. The costs of inspections for one day are roughly made up of the costs for one team of divers including equipment and renting the diving support vessel. Some reference values are presented in [Poppe, 2013; Straub et al., 2006]. The repair costs are similar to the inspection cost in that they are made up from the same costs for divers and diving support vessel. However the type of repair and number of details repaired can provide substantially different costs. In this research a differentiation is made between minor and major repairs. The minor repairs can be represented by the grinding of small defects during inspections or other non-extensive repairs can be performed with small financial costs. The major repairs are represented by actions performed with higher financial cost, like the repair of larger defects where more specialised techniques and equipment are necessary.

The chances of success for the repairs is considered in the BN by assuming a 60% and 95% chance respectively. These values are provided in the chance node $PRep_1$. If a repair is successfully performed, than the defect dimension distribution a_{t+1} and c_{t+1} for the following year are reset to the initial distribution.

3.3 *Maintenance optimization tool*

The BN described in the previous sections is implemented in the BN analysis software Hugin [Madsen et al., 2003]. A general user interface (GUI) has been implemented in Matlab for the maintenance optimization tool, which interfaces with Hugin.

The purpose of this optimization tool is to provide support for inspection and/or repair decisions, by providing the optimal strategies for the corresponding BN. The location-specific parameters of an OWT would be entered once, and saved as a new scenario. The software can then be run periodically, e.g. once a year, by updating the scenario with

recent inspection / repair outcomes, and then recalculating the optimal strategy based on this new information.

A view of the maintenance tool GUI Interface developed in the FeLoSeFI project is provided in Figure 2. On the left hand side the input values and parameters are collected: these are needed for constructing the BN for a new scenario or for updating an existing one. The choice between finding an optimal strategy or evaluating the performance of a given inspection policy is provided. The results of the calculations are given on the right hand side of the GUI in the form of different graphic representations to choose from.

Figure 3 presents the schematics of how the risk based inspection and maintenance policies are being determined. The first step in the analysis is gathering the information for the damage model. This information is hot-spot detail specific and contains details about:

- Type and geometry of the hot-spot detail
- Loading (stress) history
- Material parameters
- The stochastic parameters and their statistical distribution

From the information provided for the stochastic parameters (statistical distribution and the corresponding parameters of the assumed distribution), random values can be sampled for the parameters provided in Table 2. The crack growth for the detail considered can be

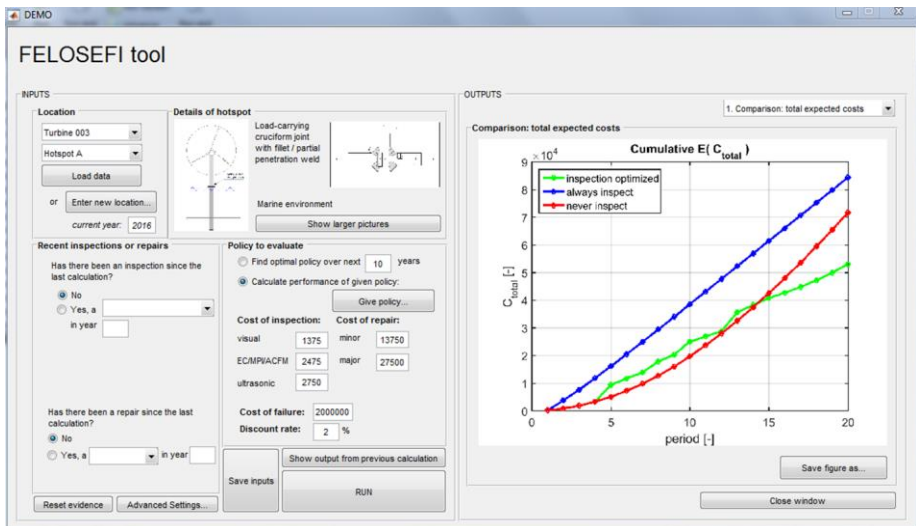


Figure 2: FeLoSeFI maintenance optimization tool GUI

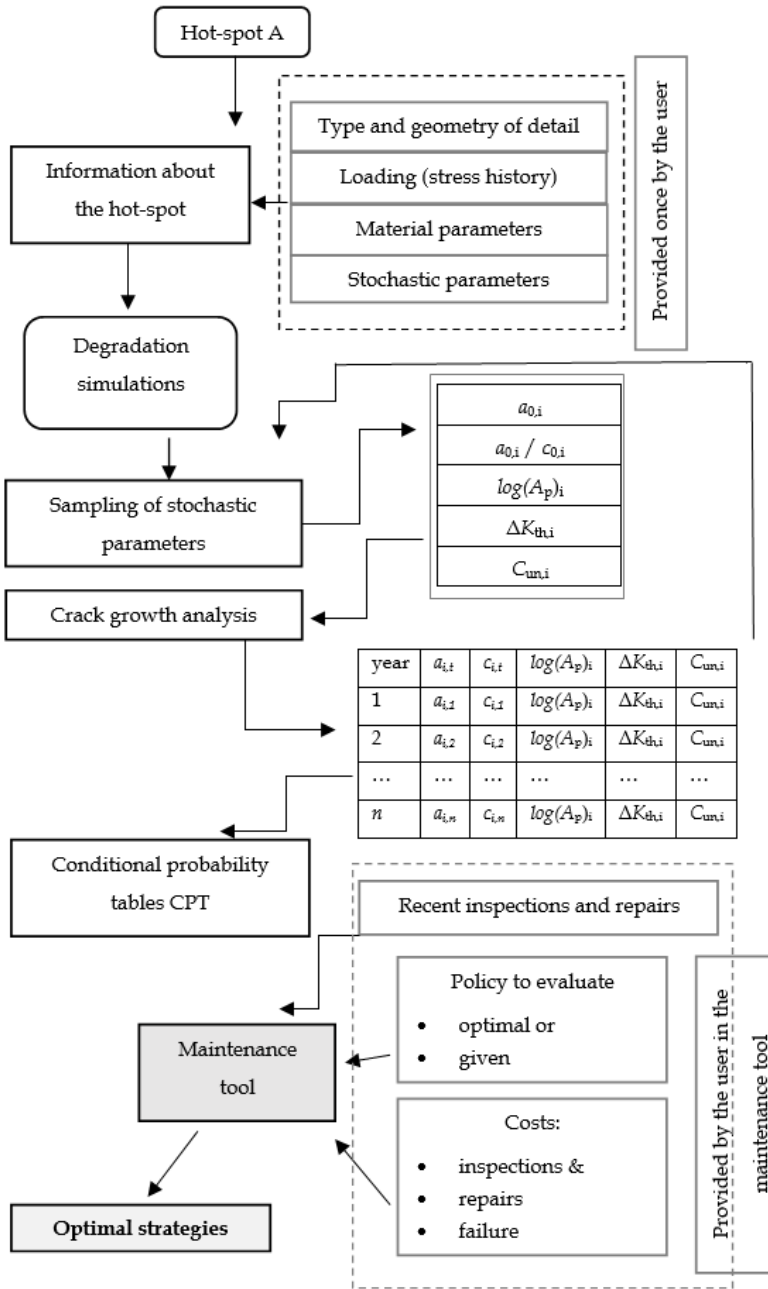


Figure 3: Schematics of the risk based inspection and maintenance policies

predicted using Fracture Mechanics based degradation models (e.g. Paris law, analytical model provided in [Dragt et al., 2020]), the state variables and external model parameters. The crack growth prediction for the design lifetime of the structure is performed and the yearly outcomes of the defect size are saved in a database. This database will then be used to quantify the relationship between the nodes by computing the conditional probability distribution for each node in the BN. Since the variables are discrete the conditional probability distributions are provided in the forms of conditional probability table (CPT). The CPT of a node in the BN is defined for a set of discrete random variables and provides the marginal probability of the considered variable in the node with respect to the variables in the nodes that lead to the considered variable. For example, consider the node for the state variable a (crack depth) in the second year. The variables that are linked to the chance node a_2 are the chance nodes $Prep_1$, a_1 , a_1/c_1 , C_{un} , ΔK_{th} and A_p . For each combination of these discrete parent variables the probability of a_2 is computed and filled in the CPT. The size of a CPT is related to the number of parent nodes and the number of discrete values of the parent nodes.

4 Examples for the application of the maintenance optimization tool

This section presents a couple of examples for the application of the Bayesian networks and maintenance tool developed in the FeLoSEFI project. Both cases look into the inspection planning for a welded detail in a monopile wind turbine support structure. The major differences between the two cases considered are related to the loading stress signal at the detail considered, the crack growth rate corresponding to the environment in which the detail is situated and the degradation model used to predict the crack growth. Table 4 provides an overview of main parameters used in the degradation model, specific for the two cases. Table 5 gives the stochastic variables (initial state variables and external model parameters) used in the degradation models. The geometry and location of the considered details are presented in Figure 4.

Part of the stress signals used is presented in Figure 5 (for example 2). For both examples, postprocessing of the original signal was necessary in order to convert it into a year equivalent signal. Furthermore, a rainflow counting based method is used in order to make the signal suitable for a cycle-by-cycle degradation model. In both examples, two situations have been considered with respect to the loading stress signal: the 1 year equivalent, cycle-

Table 4: Deterministic parameters for the degradation model

Information regarding detail	Example 1	Example 2
Flaw type	semi-elliptical surface flaw	
Weld geometry	non load-carrying or full penetration weld	
Detail geometry		
Plate thickness	30 mm	30 mm
Plate width	1000 mm	1000 mm
Attachment length	30 mm	30 mm
Weld angle	45 °	45 °
Strength parameters		
Yield stress	380 MPa	380 MPa
Ultimate stress	486 MPa	486 MPa
Modulus of elasticity	210000 MPa	210000 MPa
Poisson ratio	0.3	0.3
Fracture toughness	20600 N/mm ^{1.5}	20600 N/mm ^{1.5}
Crack growth constants		
$\log(A_{p1})$	see Table 5	see Table 5
$\log(A_{p2})$	-9.62/-6.99	-9.62
m_1	4.32/5.10	4.32
m_2	2.09/1.40	2.09
Threshold ΔK_{th}	see Table 5	see Table 5
Damage model		
Effect of retardation/acceleration	no	yes
Loading		
Loading stress signal	1 year equivalent and 1 year equivalent scaled	

-by-cycle suitable stress signal and a scaled version of the former. The signal scaling consisted of stress cycles increased/decreased by 10% with respect to the reference signal.

For the fatigue crack growth simulations, two models have been considered: one that does not take the retardation and acceleration effects into account and an analytical model developed in the FeLoSEFI project which takes the retardation and acceleration effects into account [Dragt et al., 2020].

Table 5: Stochastic parameters for the degradation model

	Distribution	Mean value	Standard deviation
Initial state variables			
Initial crack depth a_0	Lognormal	0.15 mm	0.10 mm
Initial aspect ratio a_0/c_0	Lognormal	0.62	0.25
External model parameters			
Model uncertainty parameter C_{un}	Lognormal	1.00	0.27
$\log(A_{p1})$ - air environment	Normal	-16.07	0.155
$\log(A_{p1})$ - marine environment + CP	Normal	-17.32	0.321
ΔK_{th} - air environment	Lognormal	200 N/mm ^{1.5}	80 N/mm ^{1.5}
ΔK_{th} - marine environment + CP	Lognormal	140 N/mm ^{1.5}	56 N/mm ^{1.5}

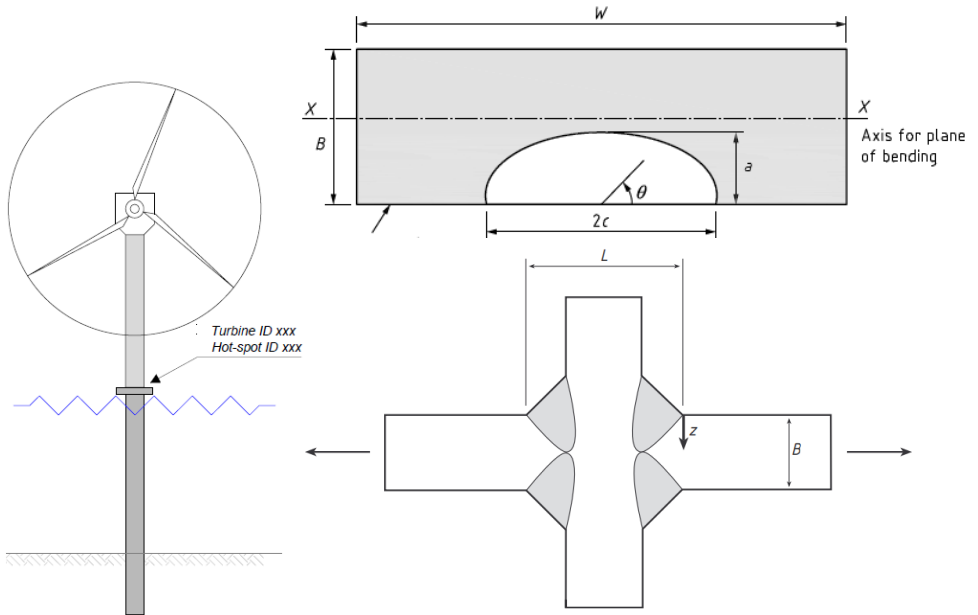


Figure 4: Location of the detail considered and type of flaw assumed in the degradation model

The first step is to create samples from the stochastic parameters provided in Table 5. These samples (initial state variables and external model parameters) are then used together with the parameters that are characteristic for the considered hot-spot detail (see Table 4) in fracture mechanics calculations to predict the crack growth of potential defects

that might be present in the details considered. This set of data is then used to fill the conditional probability tables for the nodes in the Bayesian network.

The next step is to use the maintenance tool described in section 3.3 to determine the optimal policy given the information regarding recent inspections and repairs, cost of inspection and repairs and the cost of failure. The costs used in this example are given in Table 6. The assumption is that the investment cost can be roughly estimated at € 1.23 million/MW [Krohn et al, 2009] and for a typical 2 MW wind turbine installed in Europe this yields a total investment cost of € 2.5 million. The cost of inspection is estimated provided that a maximum of 8 details can be inspected in one day, when the inspection is done in less good working conditions.

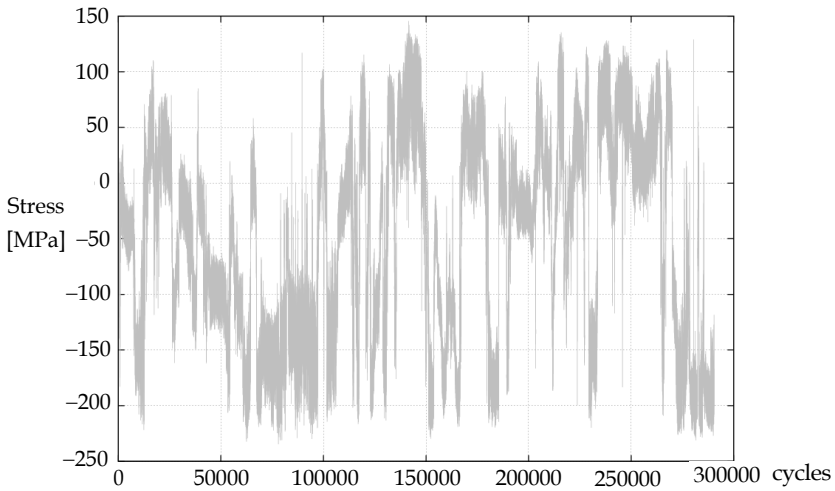


Figure 5: Stress loading signal used in example 2

Table 6: Estimated cost for inspection and repair works

Type of work	Cost per detail (€)
Inspection type	
EC / MPI / ACFM	2475
UT	2750
Visual	1375
Repair type	
Minor repair	13750
Major repair	27500

4.1 Results for simulations - example 1

For the first example several cases have been considered, listed below:

- 1 Year equivalent, cycle-by-cycle suitable stress signal and detail in air environment
- Scaled (10% increase) 1 year equivalent, cycle-by-cycle suitable stress signal and detail in air environment
- 1 Year equivalent, cycle-by-cycle suitable stress signal and detail in marine environment, foreseen with cathodic protection at -1100 mV

Three scenarios are evaluated and compared:

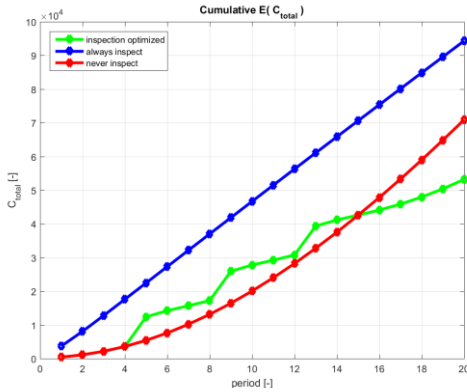
- Inspection optimized: this is the optimized inspection strategy or the inspection strategy provided by the user to be evaluated
- Always inspect: in this case an inspection is performed every year
- Never inspect: in this case there is never an inspection performed

By running the maintenance tool, an optimal strategy is derived for the first case which consists of performing 2 inspections: the first inspection after 5 years and the second after 6 years from the first inspection. After the last inspection (year 11) the periodic inspections stop due to the optimization horizon that ends at year 20. Should the inspection policy be updated regularly, by adding recent inspections/repairs and their outcome, then the optimal strategy will be updated.

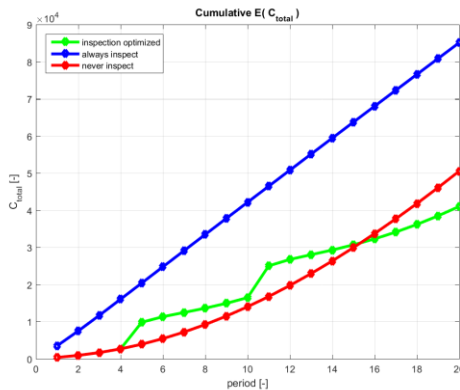
For the second case, an optimal strategy is derived which consists in performing 3 inspections: the first inspection after 5 years, the second after 4 years from the first inspection and the third inspection after 4 years from the second inspection.

For case 3, an optimal strategy is derived which consists in performing 3 inspections: the first inspection after 3 years, the second after 4 years from the first inspection and the third inspection after 5 years from the second inspection.

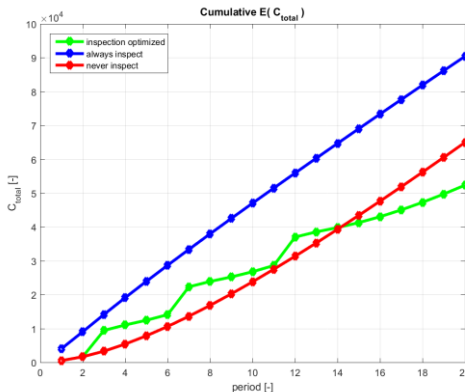
The expected total costs for different strategies ('inspection optimized' - green line, 'always inspect' - blue line, 'never inspect' - red line) and for the different cases considered are presented in Figure 6. The "always inspect" policy provides a reference line and it is not an expected inspection scenario. With respect to the first part of the design life, the "never inspect" policy and the "inspection optimized" seem to be the most beneficial one from the cost point of view. On the long run, the "inspection optimized" policy is the most cost-effective. A total cost reduction of 53% (case 1), 43% (case 2) and 42% (case 3) respectively is provided by the optimized inspection policy with respect to the "always inspect" policy.



Example 1, Case 1



Example 1, Case 2

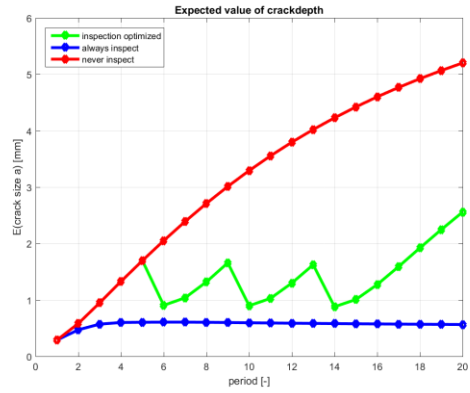


Example 1, Case 3

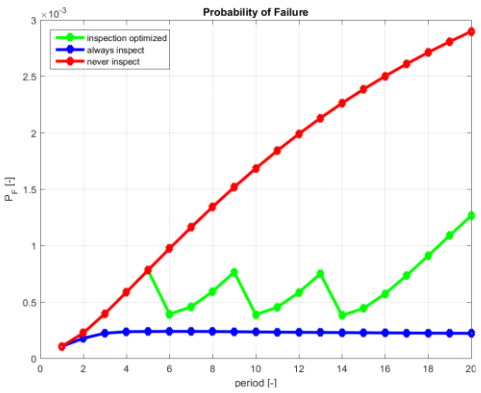
Figure 6: Cumulative costs for the different strategies over OWT lifetime (x axis in number of periods, with each period corresponding to 1 year)

With respect to the “never inspect” policy a total cost reduction of 20% (case 1 and case 3) and 23% (case 2) respectively is provided by the “inspection optimized” policy. The expected crack depth value is the average crack size of all runs and is therefore for all 3 scenarios relatively small (see Figure 7). The optimized inspection policy provides consistent low failure probabilities throughout service life (see Figure 8), in particular when compared to the “never inspect” policy. Note that the optimized policy competes with the “never inspect” policy when considering costs.

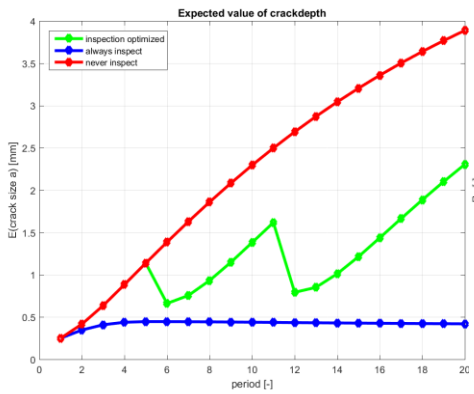
The increased number of inspections for case 2 with respect to case 1 can be related to the 10% higher stress signal amplitudes. The increase in the loading signal provides a 32% increase in total costs for the “optimized inspection” policy. The increased number of inspections for case 3 can be related to the higher crack growth rate assumed for the marine environment + CP. The defect is growing faster towards the critical defect. A higher percentage of simulations end due to reaching the critical defect before the end of the design lifetime of 20 years. The asymptote is representing the limitation of the crack growth due to reaching this critical size. Hence, although the mean value of the crack size at 20 years is in the same order of magnitude as for the original case (case 1), more inspections are found when the inspection regime is optimized due to the



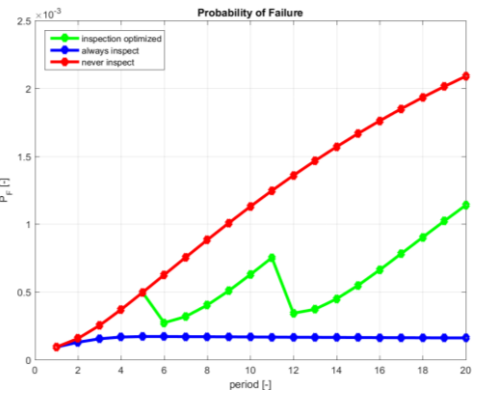
Example 1, Case 1



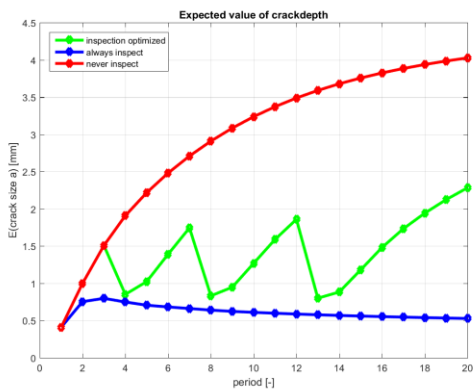
Example 1, Case 1



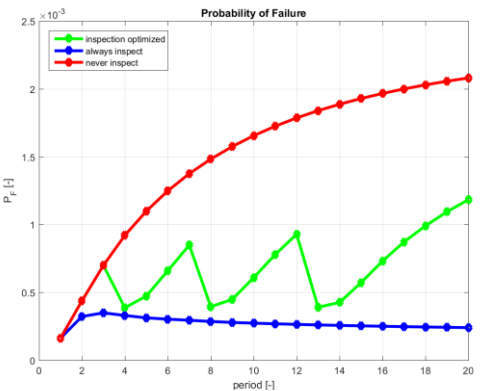
Example 1, Case 2



Example 1, Case 2



Example 1, Case 3



Example 1, Case 3

Figure 7: Expected (predicted) crack depth for the different strategies over OWT lifetime (x axis in number of periods, with each period corresponding to 1 year)

Figure 8: Probability of failure for the different strategies over OWT lifetime

fact that these values are being reached earlier in time. An increase of 30% of the total costs for the “inspection optimized” policy is needed for case 3 compared to case 1.

4.2 Results for simulations - example 2

For the second example several cases have been considered, listed below

- 1 Year equivalent, cycle-by-cycle suitable stress signal, detail in air environment and no retardation and acceleration effects considered
- 1 Year equivalent, cycle-by-cycle suitable stress signal, detail in air environment and retardation and acceleration effects considered
- Scaled (10% decrease) 1 year equivalent, cycle-by-cycle suitable stress signal, detail in air environment and retardation and acceleration effects considered.

The same maintenance scenario's as for example 1 are evaluated and compared.

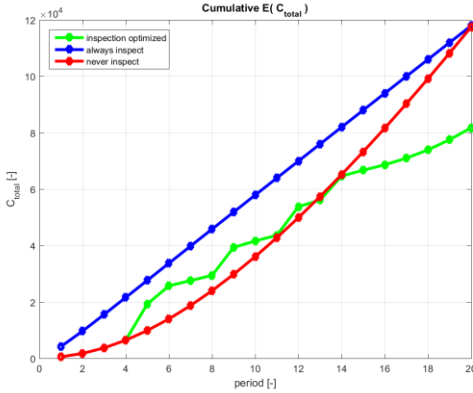
For the case when no retardation and acceleration effects are predicted, the optimal strategy is to perform an ultrasonic inspection 4 years from the date of calculation. This is followed by periodic inspections every 3 years. After 14 years no inspections are provided, given that the optimization horizon ends at 20 years.

For the second case, when retardation and acceleration effects are predicted, the same optimal strategy is found as for case 1. This is due to the negligible net effect of overloads and underloads on the entire life of the detail which can be explained by the cancelling effect of underloads after overloads.

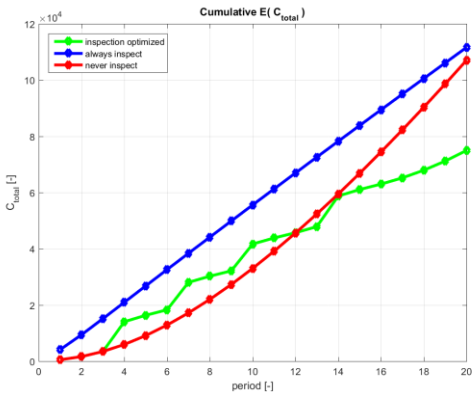
For the third case, when the signal has been scaled by reducing the stress amplitudes with 10%, the following difference can be observed with respect to the unscaled stress signal:

- Three inspections in optimized strategy, instead of four in case 1 and 2
- The first inspection 5 years from the date of calculations, the others with 4 years in between
- The total cost for the optimal strategy is 60 k Euro instead of 78 k Euro for case 1 and case 2
- The probability of failure P_f at the end of design life (for the “no inspection strategy”) is equal to $3.8 \cdot 10^{-3}$ instead of $4.2 \cdot 10^{-3}$ for cases 1 and 2

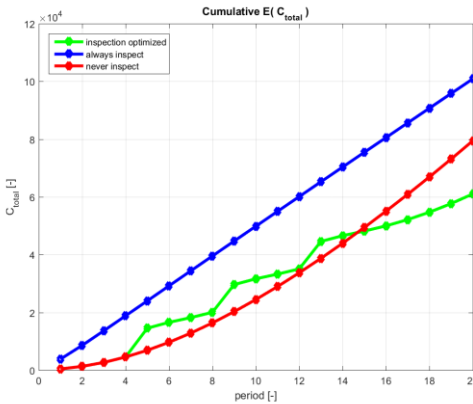
The expected total costs for different strategies (‘inspection optimized’, ‘always inspect’, ‘never inspect’) is presented in Figure 9. The ‘never inspect’ strategy is the most beneficial



Example 2, Case 1



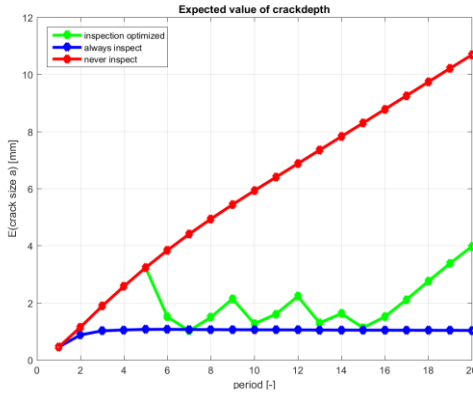
Example 2, Case 2



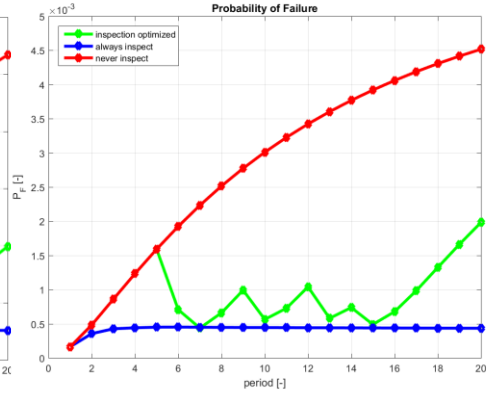
Example 2, Case 3

Figure 9: Cumulative costs for the different strategies over OWT lifetime (x axis in number of periods, with each period corresponding to 1 year)

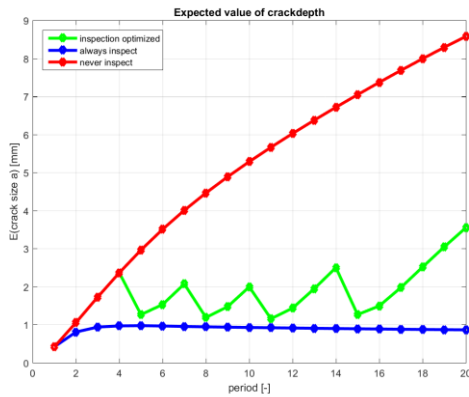
from the cost point of view in the short run, but it becomes exponentially expensive after that, due to the increasing probability of failure. The 'always inspect' strategy leads to consistently low failure probabilities (see Figure 11). The high inspection costs however lead to the highest total expected value for the costs of this strategy. The 'inspection optimized' policy there provides a 28% cost reduction with respect to the 'never inspect' policy and a 30% reduction in expected costs when compared to the 'always inspect' policy. The predicted crack depth is provided in Figure 10.



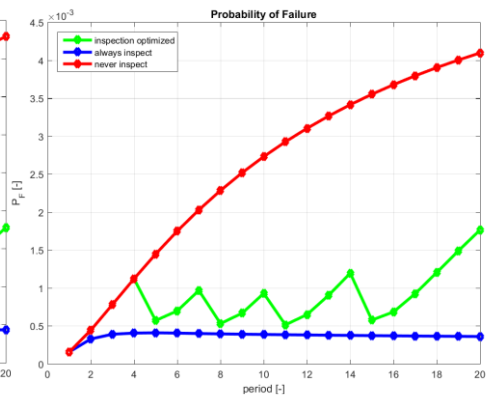
Example 2, Case 1



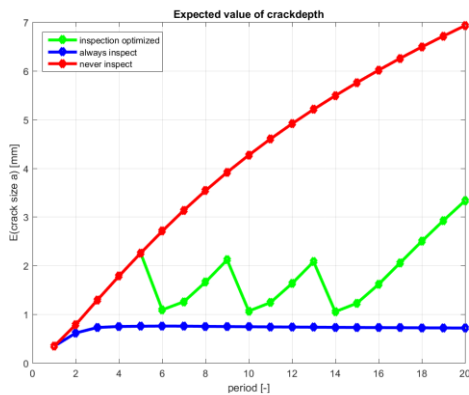
Example 2, Case 1



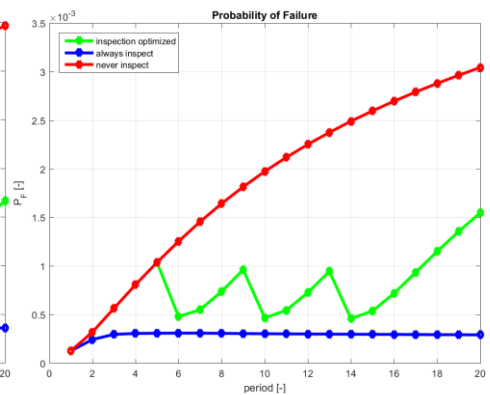
Example 2, Case 2



Example 2, Case 2



Example 2, Case 3



Example 2, Case 3

Figure 10: Expected (predicted) crack depth for the different strategies over OWT lifetime (x axis in number of periods, with each period corresponding to 1 year)

Figure 11: Probability of failure for the different strategies over OWT lifetime

5 Conclusions

This research provides a risk based tool for offshore wind turbines (OWT) for optimizing the planning and total costs of inspection and repairs. The risk based concept behind this tool takes into account the uncertainties in the degradation of OWT and finds the optimal inspection and repair strategy in order to balance the probability of failure with the costs of maintenance.

Bayesian networks are used for this risk-based planning of inspection and repairs for OWT's. These have the advantage that as soon as new information is available regarding recent maintenance works (inspection or repairs) it can be used to update the model and provide optimal maintenance strategies based also on these updates. Limited memory influence diagram (LIMID) are used in this research due to their feasibility regarding the complexity of the optimization problem and computational time. Single policy updating algorithms are used which means that the algorithm checks the performance of the strategy by changing one policy at a time.

Though the approach is mathematically complex and relative new in its application the research has shown that:

- There is a solid theoretical basis for tackling the risk based inspection (RBI) concept
- Its implementation is feasible given today's availability of commercial BN software
- The RBI concept and implementation are in agreement with strategies from the DNV guidelines
- The cases calculated are well within expected and physically comprehensible observations from practice

The implementation is performed in such a way that the actual crack growth behaviour is prepared beforehand and stored in a data base. This benefits the flexibility of the tool as it can address different databases instead of having to perform dedicated crack growth calculations each time a different model is to be chosen. The Graphical User Interface furthermore enables the user specific dedicated input with respect to inspection types, repair methods and associated costs.

The first example presented showed the impact of increased loading through stress levels and environmental conditions (air/marine environment). For each condition the

methodology derived cost optimal inspection regimes. Compared to a yearly inspection policy, these cost savings are in the order of 50% and 40% for respectively the nominal and the two cases with increased loading conditions.

In the second example, the effect of retardation and acceleration as well as the effect of lowering the stress levels is investigated. Consistent results were found, with negligible effects of retardation and acceleration (cancelling effects) on lower costs and less inspections when the loading was decreased.

The example cases presented show that specific knowledge with respect to, for instance, actual loading reduces uncertainties and has a direct impact on the inspection policies. The tool thus enables the recalculation of new scenarios based on monitoring data showing the value of monitoring.

Literature

- BS7910:2013+A1:2015, Guide to methods for assessing the acceptability of flaws in metallic structure, BSI, 2015.
- Chryssanthopoulos, M., Righiniotis, T., Fatigue reliability of welded steel structures, *Journal of Constructional Steel Research* 62, p. 1199–1209, 2006.
- DNV-GL, DNVGL-RP-C210 Probabilistic methods for planning of inspection for fatigue cracks in offshore structures, DNV-GL, 2015.
- Dragt, R.C., Hengeveld, S.T., Maljaars, J., Analytical prediction model of crack growth retardation and acceleration, *HERON* Vol. 65 (2020) No. 1/2, pp. 109-149.
- Faber, M., Vrouwenvelder, A., Probabilistic model code. Joint Committee on Structural Safety, 2001.
- Kjaerulff, U.B., Madsen, A.L., *Bayesian networks and influence diagrams*, Springer Science, 2008.
- Krohn, S., Morthorst, P.-E., Awerbuch, S., *The Economics of Wind Energy*, A report by the European Wind Energy Association, EWEA, 2009.
- Lauritzen, S.L., Nilsson, D., Representing and solving decision problems with limited information. *Management Science* 47, p. 1235–1251, 2001.

- Madsen, A., Lang, M., B. Kjærulff, U., Jensen, F., The Hugin Tool for Learning Bayesian Networks. Lecture Notes in Artificial Intelligence (Subseries of Lecture Notes in Computer Science), 2003.
- Maljaars, J., Steenbergen, H., Vrouwenvelder, A., Probabilistic model for fatigue crack growth and fracture of welded joints in civil engineering structure, *International journal of fatigue* 38, p. 108-117, 2012.
- Nielsen, J.J., Sørensen, J.D., *Risk-based operation and maintenance of offshore wind turbines using Bayesian networks, Applications of Statistics and Probability in Civil Engineering*, Taylor & Francis Group, London, 2011.
- Poppe, T., Periodic inspection Experience on Alpha Ventus - presentation at EWE conference, Hamburg, 2013.
- Straub, D., Goyet, J., Sørensen, J., Faber, M., Benefits of Risk Based Inspection Planning for Offshore Structures, Proceedings of the *International Conference on Offshore Mechanics and Arctic Engineering - OMAE*, 2006.
- Straub, D.M., Stochastic modeling of deterioration pro-cesses through dynamic Bayesian networks. *Journal of Engineering Mechanics*, Trans. ASCE, 2009, 135(10): p. 1089-1099, 2009.